3D of Brain Shape and Volume After Cranial Vault Remodeling Surgery for Craniosynostosis Correction in Infants

Beatriz Paniagua*[a], Omri Emodi[b], Jonathan Hill[b], James Fishbaugh[c], Luiz A Pimenta[d], Stephen R. Aylward[e], Enquobahrie Andinet[e], Guido Gerig[c], John Gilmore[a], John A van Aalst[b], Martin Styner[a]
[a]Department of Psychiatry, University of North Carolina at Chapel Hill; [b]Department of Plastic Surgery, University of North Carolina at Chapel Hill; [c]Scientific Computing Institute, University of Utah; [d]Department of Dentistry, University of North Carolina at Chapel Hill; [e]Kitware, Inc.

ABSTRACT

The skull of young children is made up of bony plates that enable growth. Craniosynostosis is a birth defect that causes one or more sutures on an infant's skull to close prematurely. Corrective surgery focuses on cranial and orbital rim shaping to return the skull to a more normal shape. Functional problems caused by craniosynostosis such as speech and motor delay can improve after surgical correction, but a post-surgical analysis of brain development in comparison with age-matched healthy controls is necessary to assess surgical outcome. Full brain segmentations obtained from pre- and post-operative computed tomography (CT) scans of 8 patients with single suture sagittal (n=5) and metopic (n=3), non-syndromic craniosynostosis from 41 to 452 days-of-age were included in this study. Age-matched controls obtained via 4D acceleration-based regression of a cohort of 402 full brain segmentations from healthy controls magnetic resonance images (MRI) were also used for comparison (ages 38 to 825 days). 3D point-based models of patient and control cohorts were obtained using SPHARM-PDM shape analysis tool. From a full dataset of regressed shapes, 240 healthy regressed shapes between 30 and 588 days-of-age (time step = 2.34 days) were selected. Volumes and shape metrics were obtained for craniosynostosis and healthy age-matched subjects. Volumes and shape metrics in single suture craniosynostosis patients were larger than age-matched controls for pre- and post-surgery. The use of 3D shape and volumetric measurements show that brain growth is not normal in patients with single suture craniosynostosis.

Keywords: Pediatric neuroimaging, plastic Surgery, shape regression, volumetric analysis, shape analysis

1. INTRODUCTION

The skull of young children is made up of bony plates that allow for its growth. Craniosynostosis is a birth defect that causes one or more sutures on an infant's skull to close earlier than normal, causing abnormal head shape in infants. It has a prevalence of approximately 3.5 to 4.5 per 10,000 live births [1]. In the 19th century, craniosynostosis was treated by strip craniotomy; by the 1950s treatment involved total cranial vault reconstruction. Over the last 25 years, surgery has focused on cranial and orbital rim shaping to return the calvarium to a "normal" shape. Over the last 10 years, there has been a reversion to less invasive techniques including endoscopic strip craniotomy with helmet remolding and spring-driven distraction [2].

There are numerous types of craniosynostosis. Different names are given to the various types, depending on which suture, or sutures, are involved, including the following:

- Sagittal craniosynostosis (figure 1a) involves an early closure of fusion of the sagittal suture. This suture runs front to back, down the middle of the top of the head. This fusion causes a long, narrow skull. The skull is long from front to back and narrow from ear to ear.
- Metopic craniosynostosis (see figure 1b) is a fusion of the metopic (forehead) suture. This suture runs from the top of the head down the middle of the forehead, toward the nose. Early closure of this suture may result in a prominent ridge running down the forehead, as well as abnormally close eyes (hypotelorism).

For unknown reasons, a diagnosis of sagittal synostosis predominated in large series, but more recently has been replaced by metopic synostosis. The etiology of craniosynostosis is explained in two different theories introduced by Virchow et al. [3] and Moss et al. [4]. The Virchow theory is that primary suture fusion causes brain deformity and brain

Medical Imaging 2013: Biomedical Applications in Molecular, Structural, and Functional Imaging,
edited by John B. Weaver, Robert C. Molthen, Proc. of SPIE Vol. 8672, 86720V

growth parallel to the suture fusion. The Moss theory "functional matrix" is that the suture fusion is secondary to abnormal brain growth. Moss was the first clinician to introduce the idea that contemplates the fact the sutures will close early if there are no growing forces motivated by the brain.

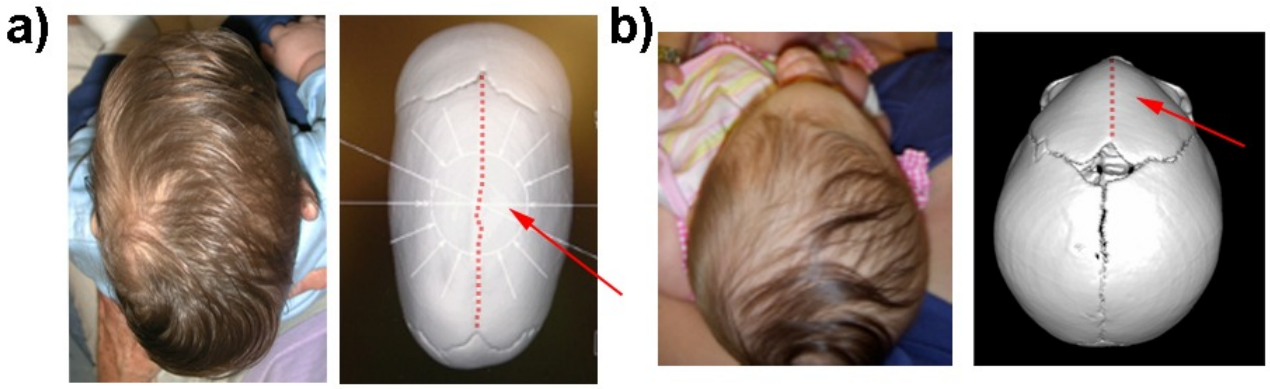

Figure 1. Clinical pictures and 3D models of skulls from infants with single suture craniosynostosis. The red dashed line indicates where the closure occurs a) Sagittal suture closure b) Metopic suture closure

Functional problems caused by craniosynostosis such as speech and motor delay improve after surgical correction, but a post-surgical analysis of brain development in comparison with age-matched healthy controls is necessary to assess surgical outcome. Today single suture synostosis is detected by clinical evaluation of head shape, head circumference and radiological assessment via CT and skull radiographs (Rx). Both CT and skull Rx are evaluations done by clinicians on 2D information. There is obviously a problem of judgment due to the fact doctors are trying to diagnose a problem in 3D with 2D tools.

Even with the progressive evolution to less-invasive surgical techniques, craniosynostosis surgical correction is a invasive procedure that happens early in life (usually in infants between 3 and 9 months-old). After surgery the cranial shape goes back to normal, but the structure of the skull of the infant after surgery changes permanently (see figure 2) so it is necessary to fully understand the morphological changes happening in nonsyndromic craniosynostosis.

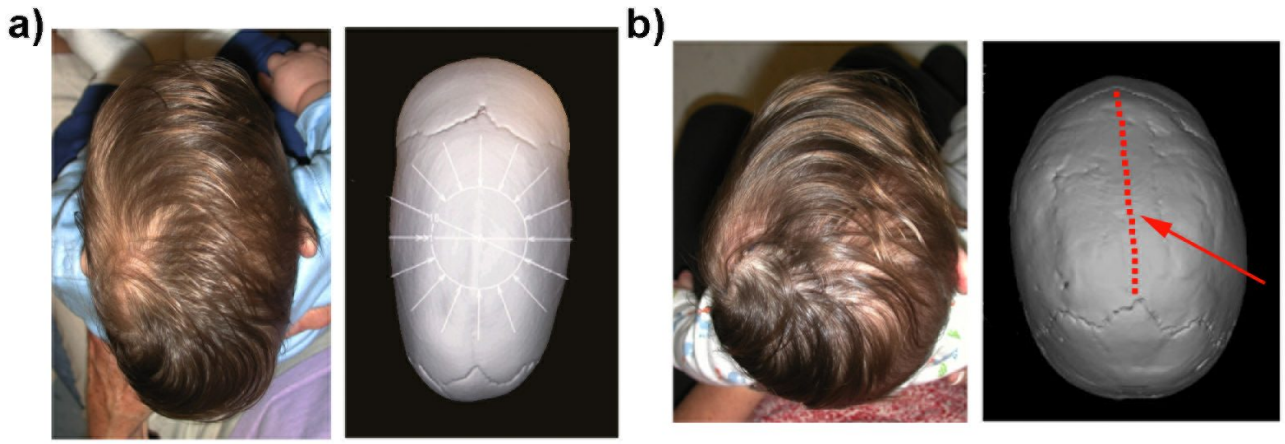

Figure 2. Clinical pictures and 3D models of skulls from one infants with sagittal single suture craniosynostosis a) before and b) after surgery. The red dashed line indicates that despite of being a normal skull, the cranium of the patient is still missing the sagittal suture.

This study tries to find a computerized automatic evaluation of brain growth in infants, pre- and post- surgical correction of single suture craniosynostosis. In addition to that we aim to demonstrate that brain growth is not normal following calvarial surgery in patients with single suture craniosynostosis, following the ideas first introduced by Moss et al. [4]. We plan to test our hypothesis using a cohort of patients with these two types of synostosis, compared with subjects that

have a healthy developing brain. Through these patients we would like to determine reliable, reproducible means of following brain growth after calvarial vault remodeling.

To this end, the paper is structured as follows: in section 2 "Materials" the imaging data and the acquisition scan parameters are described. Section 3 "Methods" explains each one of the methodological steps followed in this study, consisting in: full brain segmentation ("Full brain segmentation"), validation of CT versus MRI full brain segmentation (in "Full brain segmentation validation"), computation of full brain correspondent point-based models for healthy and craniosynostosis subjects via SPHARM-PDM toolbox ("SPHARM-PDM"), construction of a 4D healthy growth trend via acceleration-controlled shape regression ("Shape Regression") and calculation of shape and volume metrics to compare healthy and craniosynostosis patients ("Shape and volume metrics computation"). Section 4 "Results" describes the results obtained in the quantification of volumetric and shape differences between healthy and craniosynostosis subjects, while section 5 "Discussion" has the conclusion and discussion points.

2. MATERIALS

Computed tomographic (CT) scans of all single suture craniosynostosis (n=8) were used in this study. Metopic and sagittal craniosynostosis patients were scanned pre- and post-surgically between 1 month and 2 years of age. Syndromic patients and patients with other sutures than metopic or sagittal were excluded. Scans were helical multidetector CT, using a slice thickness of 0.316x0.316x2 mm. All scans were resized to isotropic 1 mm voxel dimension for the analysis. A group of 402 healthy controls magnetic resonance images (MRI) were used for comparison (ages 38~825 days). Images were acquired on a Siemens 3T scanner (Allegra, Siemens Medical System, Erlangen, Germany). Infants were scanned unsedated while asleep, fitted with ear protection and had their heads secured in a vacuum fixation device at both 1 and 2 year follow up sessions. T1-weighted, proton density and T2-weighted images were obtained. Spatial resolution was 1x1x1 mm for T1-weighted images, 1.25x1.25x1.5 mm with .5 mm gap for PD/T2-weight images.

3. METHODS

3.1 Full brain segmentation

Segmentation of craniosynostosis CT scans was performed via automatic tissue classification based in Hounsfield Units. Automatically classified cranio Cerebro Spinal Fluid (CSF), white and grey matter labels were extracted, merged and manually post-processed for the extraction of a full brain mask. For all healthy MRI datasets, full brain segmentation was performed using AutoSeg [5] that is a tool allowing the segmentation of probabilistic sub-cortical structures and label maps, such as generic ROI maps and parcellation maps. The approach is a fully automatic segmentation via a deformable registration of an unbiased diffeomorphic atlas with probabilistic spatial priors. Post-processing with 3D connectivity, morphological closing and minor manual editing provided simply connected 3D objects.

3.2 Full brain segmentation validation

Due to the different nature of the CT and MRI image modalities and segmentation techniques, a validation study to compare inter-modality variability was performed. Both MRI and CT were acquired for the same subject at ages (age in days) and (age in days), respectively. Segmentation for MRI and CT was performed as described above. Figure 3 shows sagittal, coronal and axial cross-sections with 3D surfaces rendered for both CT (red) and MRI (green), with slice interserction visibles in the image data. Red and green line show no bigger differences a voxel from each other. When comparing volumetric measurements between MRI and CT segmentation, differences are negligible (MRI = 1.5823 x 106 mm3 and CT = 1.5579 x 106 mm3 difference = 1.54%). We can conclude we can reliably compare full brain masks extracted from both MRI and CT image modalities.

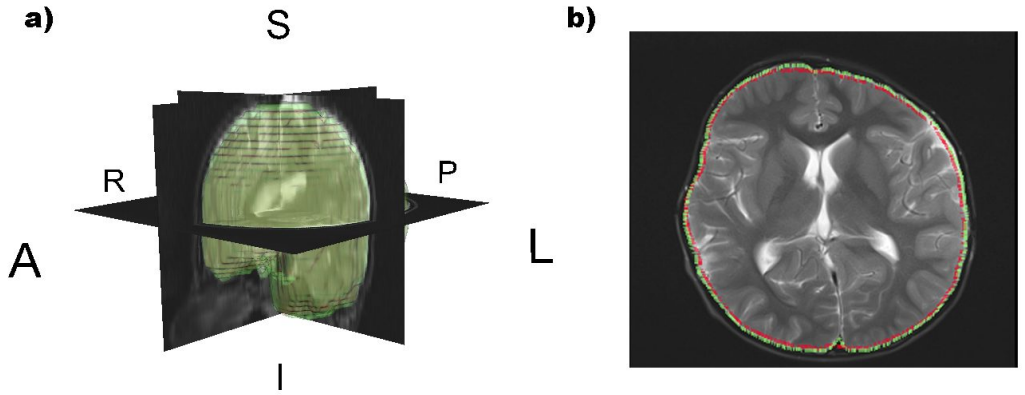

Figure 3. CT-MRI segmentation validation a) Semi-transparent overlay of the 3D full brain surfaces from CT (red) and MRI (green) showing almost no changes b) MRI coronal slice displaying surface intersections with CT (red) and MRI (green) showing changes no bigger than one voxel

3.3 SPHARM-PDM

We performed a local shape analysis on the lateral ventricle segmentations via the UNC SPHARM-PDM (Spherical HARMonics Point Distribution Models) shape analysis toolbox. The SPHARM-PDM toolbox presents a comprehensive set of tools for the computation of 3D structural statistical shape analysis. The SPHARM-PDM description is a sampled boundary description with object-inherent correspondence that can only represent objects of spherical topology [6]. The input of SPHARM-PDM toolbox is our set of full brain segmentations. These segmentations are first processed to ensure spherical topology and then converted to surface meshes. Next, a spherical parameterization is computed from the surface meshes using an area-preserving, distortion minimizing spherical mapping. Further, the SPHARM description is computed from the mesh and its spherical parameterization [7]. The correspondence is determined by aligning the principal curves of first order ellipsoid representation with the standard coordinate frame, so that the north pole of the first order ellipsoid aligns with the positive z axis, and its 0° meridian aligns with the x–z plane. This description is then sampled into triangulated surfaces via an icosahedron subdivision of the spherical parameterization. Full brain surfaces are well represented (local representation error is smaller than 0.1 mm on average) by a subdivision of level 20 resulting in 4002 surface points. Alignment of triangulated surfaces was finally performed using rigid body, Generalized Procrustes alignment that iteratively aligns the surfaces to the population mean. By following this set of steps SPHARM-PDM creates a more uniform representation than the one obtained directly from sampling the binary segmentation into triangulated surfaces.

3.4 Shape Regression

Due to the need of accurately age-matched controls for the craniosynostosis subjects, calculating the continuous growth evolution of healthy full brain shapes is then the starting point for any further analysis. The subjects in the healthy population are used as input for the construction of a 4D atlas using acceleration-based shape regression [8]. In recent years, the scientific community has demonstrated a growing interest in longitudinal computational anatomy (i.e. construction of computer models of anatomical evolution). 4D continuous growth models provide a tool to generate shapes at any instant in time (within the interval defined by the data), offering us the opportunity to continuously measure shape properties. Computer models of anatomical evolution, such as the 4D full brain atlas constructed for this study via acceleration-controled shape regression, estimate growth trajectories. Shape regression involves inferring the continuous evolution of shape to closely match a set of target shapes over time. The problem is often posed as the trade off between fidelity to data and regularity; with the most likely shape evolution estimated based on a regularized least-square criterion [8].

Acceleration-controlled shape regression is a shape regression method that overcomes the problems of non-smooth shape evolutions that existed in previous studies [9][10][11]. This shape regression model computes a new growth model parameterized by acceleration that provides a shape evolution model that is smooth in both space and time and that represents more closely the growth in anatomical structures. In addition, the constructed model yields a growth evolution with improved regularity, thus discarding more noise from the data to fit a more realistic growth trajectory.

Briefly, acceleration-based regression considers a discrete set of shapes S_{ti} observed at times t_i. The growth model is going to be estimated by continuously deforming an initial shape or baseline S_0 to closely match the rest of the observed shapes. The resulting shape out of continuously deforming S_0 with a transformation is expressed as $R_t = \varphi_t(S_0)$. Shape regression is then a trade off between data-matching and regularity. While the regularity is controlled with an acceleration parameter, the shape similarity metric is obtained by modeling each one of the shapes in the ensemble as currents [12]. The current-based similarity metric enforces structural integrity of the two surfaces, penalizing geometric and spatial mismatch. The shape regression method used is acceleration-controlled regression and it is further described in [8][13].

Therefore, shape regression is a tool we use to generate healthy brain shapes at any instant in time (within the interval defined by the data), offering us the opportunity to continuously measure shape properties. Any desired measurement can simply be extracted from the collection of regressed shapes. 350 full brain shapes (see figure 4) were obtained between 6 and 825 days of age (time step = 2.34 days). For the final analysis only 240 regressed shapes between 30 and 588 days of age were included in the study.

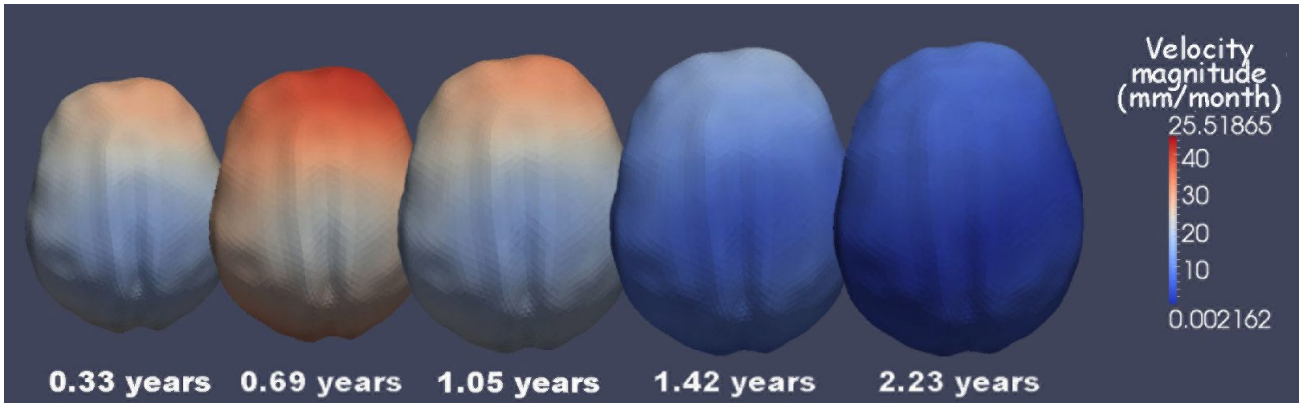

Figure 4. Five snapshots of healthy average brain shape evolution from 3 months-old to 26 months-old (0.33 years-old to 2.23 years-old, left to right). The color denotes magnitude of velocity. The brain evolution shows a more rapid growth at younger age, that occurs along the anterior/posterior axis.

3.5 Shape and volume metrics computation

Volumes and shape metrics were obtained for craniosynostosis and healthy age-matched subjects obtained by shape regression. Craniosynostosis and healthy subject surface-to-surface distances with healthy regressed shapes were computed using MeshValmet 2.1 [14]. MeshValmet is a tool that measures surface-to-surface distance between two triangle meshes using user-specified uniform sampling, providing useful histogram and statistical information based on the sample errors. Specifically mean face distance between each subject and their age-matched regressed full brain shape will be used.

$$\overline{f} = \frac{\left(\sum_i f_i * a_i\right)}{\sum_i a_i} \tag{1}$$

For each triangle formed by neighboring samples, the error at the vertices is averaged to obtain a single error for the sample triangle. The overall mean error is obtained by calculating the mean of the errors of the sample triangles. In a triangle i with area a_i and with values at the vertex (sample points) e_{i1}, e_{i2} and e_{i3} and using linear interpolation to obtain the values within the triangle, the FaceMean value (i.e. integral of the value divided by the surface, see equation 1) is $f_i = e_{i1}+e_{i2}+e_{i3}$; the absolute mean value is $|f_i| = |e_{i1}|+|e_{i2}|+|e_{i3}|$.

4. RESULTS

Volumetric findings show enlarged full brain volumes of craniosynostosis patients pre- and post- surgical correction. Figure 5 shows in the bold black line the average volume of healthy full brains and the two regular black lines show healthy variation within the healthy cohort. All 8 craniosynostosis patients independently of gender, age, and type of single suture craniosynostosis show brain volume enlargement, compared with healthy subjects.

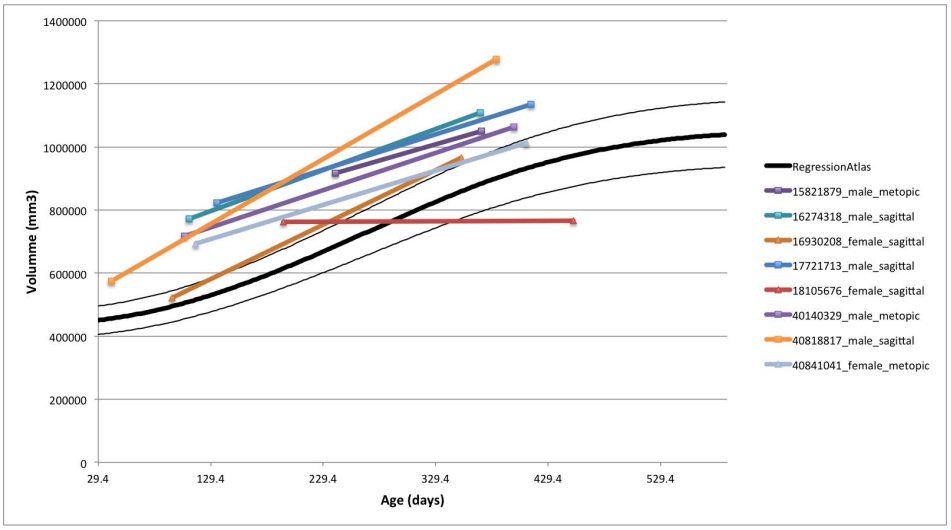

Figure 5. Volumetric findings show enlarged full brain volumes of craniosynostosis patients pre- and post- surgical correction

Craniosynostosis corrective surgery improves full brain volume, figure 5 shows that volume differences between healthy population and craniosynostosis patients decrease in the post-surgical scan.

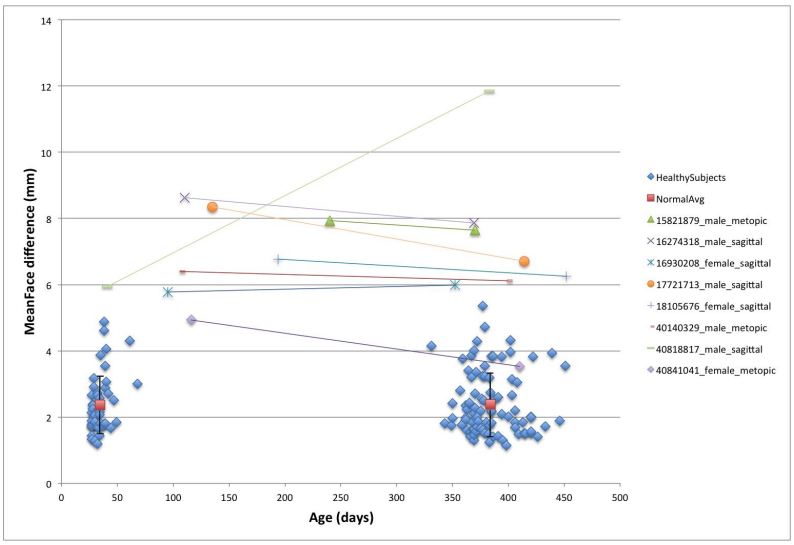

Figure 6. Shape findings show bigger surface FaceMean differences between craniosynostosis patients and healthy age matched controls, pre- and post- surgical correction.

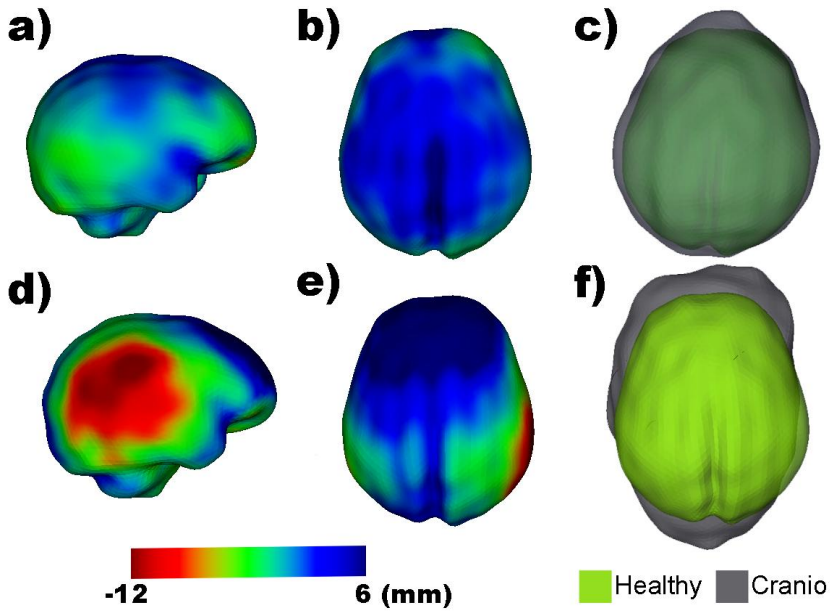

Figure 7. Shape findings displaying closest point signed distances between a metopic (a, b, c, age = 110 days) and sagittal (d, e, f, age = 116 days) craniosynostosis patients and their age-matched healthy controls. Closest Point surface distances accurately capture deformation features in both single suture craniosynostosis types.

Figure 6 shows that the shape findings concur with the volumetric findings. All craniosynostosis patients have bigger shape differences with the regressed age-matched average brains than their healthy peers. Again, we see that the existing shape differences between craniosynostosis patients and age-matched healthy subjects decrease in the post-surgical scans, indicating the necessity of craniosynostosis corrective surgery. Figure 7 shows two illustrative example of the two types of single suture craniosynostosis individual shape results for further clarification. Closest Point surface distances accurately capture deformation features in both single suture craniosynostosis types. Metopic craniosynostosis cases display a similar head circumference to healthy controls only different by the metopic ridging in the anterior part, but still have enlarged brain volume (figure 7 a), b) and c)). Sagittal craniosynostosis brain shapes have larger head circumference by elongation of the brain shape in the anterior-posterior axis and narrowing of the brain in the left-right axis (figure 7 d), e) and f)).

5. CONCLUSIONS

Volumes and shape metrics in the single suture craniosynostosis patients were larger than age-matched controls for both pre- and post-surgery. The use of 3D shape and volumetric measurements show that brain growth is not normal in patients with single suture craniosynostosis. While understanding of what causes craniosynostosis is still evolving, it does seem clear after 3D shape and volume analysis that surgical correction for craniosynostosis demonstrates to improve the brain differences between craniosynostosis patients and healthy controls.

When only one suture is fused, it is likely that only one surgery will be required to correct the abnormal skull shape. However, this pilot study demonstrates that full brain shape is abnormal pre- and post-surgical correction for both metopic and sagittal single suture craniosynostosis patients, indicating the brain in these infants differs from the normal population. Future work includes increasing our craniosynostosis cohort, including new shape metrics and using a different image modality that would allow for looking at the brain (i.e. MRI). Statistical analysis of bigger of metopic and sagittal groups of patients will help to understand the heterogeneity of the patient cohort.

REFERENCES

[1] Kolar J. C., "An Epidemiological Study of Nonsyndromal Craniosynostoses," Journal of Craniofacial Surgery, 22 , 47-49 (2011).

[2] Clayman M.A., Murad, G.J., Steele, M.H., Seagle, M.B. and Pincus, D.W., "History of craniosynostosis surgery and the evolution of minimally invasive endoscopic techniques: the University of Florida experience," Ann Plast Surg., 58, 285-7 (2007).

[3] Virchow R., "Ueber den Cretinismus, namentlich in Franken, und über pathologische Schädelformen," Verh Physikalisch Med Ges Würzburg, 2, 230-71 (1851).

[4] Moss M. L., Young, R. W., "A functional approach to craniology," Am. J. Phys. Anthropol., 18, 281–292 (1960)

[5] Vachet C., Perrot, E. and Ouziel, C., "Autoseg 2.1," http://www.nitrc.org/projects/autoseg/, (31 October 2012)

[6] Styner M., Oguz, I., Xu, S., Brechbuhler, C., Pantazis, D., Levitt, J., Shenton, M. and Gerig, G. "Framework for the Statistical Shape Analysis of Brain Structures using SPHARM-PDM," Open Science Workshop at MICCAI published at Insight Journal, DSpace link: http://hdl.handle.net/1926/215 (2006).

[7] Brechbuhler C., Gerig, G. and Kubler, O., "Parameterization of colsed surfaces for 3D shape description," Computer Vision and Image Understanding, 61(2), 154-170 (1995).

[8] Fishbaugh J., Durrleman, S. and Gerig, G. "Estimation of smooth growth trajectories with controlled acceleration from time series shape data," International Conference on Medical Image Computing and Computer Assisted Intervention, 14, 401-8 (2011).

[9] Craene M.D., Camara, O., Bijnens, B.H., Frangi, A.F. "Large diffeomorphic FFD registration for motion and strain quantification from 3D-US sequences," FIMH '09 Proceedings of the 5th International Conference on Functional Imaging and Modeling of the Heart, 5528, 437–446 (2009).

[10] Durrleman S., Pennec, X., Trouvé, A., Gerig, G., Ayache, N. "Spatiotemporal atlas estimation for developmental delay detection in longitudinal datasets," International Conference on Medical Image Computing and Computer Assisted Intervention, 5761, 297–304 (2009).

[11] Ehrhardt J., Werner, R., Schmidt-Richberg, A., Schulz, B., Handels, H. "Generation of a mean motion model of the lung using 4D-CT image data," Proc. of Eurographics Workshop on VCBM, 69–76 (2008)

[12] Vaillant M., Glaunès, J. "Surface matching via currents," IPMI 2005, 3565, 381–392 (2005)

[13] Fishbaugh J., Durrleman, S., Piven, J., and Gerig, G. "A framework for longitudinal data analysis via shape regression," Proc. of SPIE Medical Imaging, Image Processing, 8314, (2012)

[14] Paniagua B., Styner, M., Xiao, P., Xu, S., "MeshValmet 2.1," http://www.nitrc.org/projects/meshvalmet/, (31 October 2012).